Pharmaceutical Research, Vol. 25, No. 4, April 2008 (© 2007)
DOI: 10.1007/s11095-007-9375-4

Research Paper

Simultaneous FTIR Spectroscopic Imaging and Visible Photography to Monitor Tablet Dissolution and Drug Release

Sergei G. Kazarian[1,3] and Jaap van der Weerd[2]

Received March 31, 2007; accepted June 6, 2007; published online July 6, 2007

Purpose. Previous studies of hydroxypropyl methylcellulose (HPMC)-based tablet during exposure to water showed a number of 'fronts' moving into the tablet but led to contradictory interpretations. These fronts are related to water penetration into and dissolution of the tablet, but the exact nature can not be derived from visible photographic evidence. A method to study tablet dissolution simultaneously by Fourier transform infrared-attenuated total reflection (FTIR-ATR) imaging and macro-photography can assist in providing correct interpretation of the observed fronts.
Methods. Therefore, the combination of macro-photography and FTIR-ATR spectroscopic imaging was developed and used to interpret the physical changes leading to the observed fronts. Buflomedyl pyridoxal phosphate (BPP), a coloured drug, was used as a model drug.
Results. The quantitative results obtained by FTIR-ATR imaging enabled the attribution of the three observed fronts (inside to outside) to: (1) true water penetration, possibly combined with (partial) dissolution of buflomedyl pyridoxal phosphate (BPP); (2) total gellification of HPMC; (3) erosion front.
Conclusions. The method to study dissolution of a tablet simultaneously by FTIR-ATR imaging and macro-photography has been developed and used to obtain reliable interpretation of the fronts observed during tablet dissolution.

KEY WORDS: ATR; controlled release; dissolution; drug release; FT-IR imaging; gel; hydroxypropyl methylcellulose; multivariate analysis; visible photography.

INTRODUCTION

In recent years, a number of new approaches have been reported to study the behaviour of pharmaceutical tablets during dissolution. These studies aim to generate an understanding of the processes involved in a dissolving tablet. This is a welcome addition to the standard dissolution tests, which obtain the amount of dissolved active ingredient as a function of time, but do not provide information on the underlying mechanisms of tablet dissolution.

The new approaches to study tablet dissolution are mainly based on imaging (see Table I for an overview). A tablet is imaged during dissolution using a technique that can characterise important properties.

The experimental set-ups, applied samples, and information content of the results are normally dissimilar, and some aspects will be described below.

An advantage of MRI is the ease of sampling. A slice or line can be selected in a tablet completely immersed in the dissolution fluid, as MRI is a 3D technique. The other techniques can only handle two dimensions. As a result, the exposure to water has to be restricted, e.g. by means of windows, to two dimensions. The third dimension is now used to look at, or through, the sample. Such an approach is by its nature sensitive to surface effects, for example the leaking of water along the window instead of through the tablet. MRI is not affected by this leaking.

A drawback of (non-spectroscopic) MRI studies is the low chemical sensitivity and the resulting problems with quantification. Normally, the solid tablet matrix is not observed in NMR; rather, the water content is analysed and the matrix concentration is derived. Drugs can only be quantified if a special label is used, e.g. fluorine (2). However, complete quantification is not possible with (non-spectroscopic) MRI. The same applies to optical photography. Quantification has been explored by including coloured drugs, but the accuracy of the quantification can be seriously questioned, as it is hardly possible to account for the changing scattering properties of the medium due to the intake of water and gel formation. In any case, water itself is invisible in this approach. Nevertheless, the results published for photography are very interesting. They normally show a number of boundaries that steadily migrate into the tablet. Colombo and colleagues (6) recognise three different boundaries, which are named (from the inside to the outside of the tablet):

- glass transition boundary: glassy material is transformed to a gel matrix
- drug diffusion boundary: the drug dissolves and starts diffusing

[1] Department of Chemical Engineering, Imperial College London, London, SW7 2AZ, UK.
[2] *Present address:* Microtraces Section, Netherlands Forensic Institute, P.O. Box 24044 2490 AA, The Hague, The Netherlands.
[3] To whom correspondence should be addressed. (e-mail: s.kazarian@imperial.ac.uk)

Table I. Some Imaging Techniques Used for Tablet Characterisation and their Properties

Technique	Advantages	Disadvantages	References
MRI	Versatile (tablet size/form) Surface insensitive	Not quantitative Low sensitivity	1–4
VIS photography	Time resolution Inexpensive	Surface sensitive Not quantitative	5–9
Fluorescence imaging	Time resolution Specificity	Surface sensitive	10,11
ATR-FTIR imaging	Quantitative	Surface sensitive	12–17
Transmission-FTIR imaging	Quantitative	Unrealistic tablet needed (thickness <20 μm)	18
Cryo-SEM	High spatial resolution	Destructive sample preparation	19,20

MRI: magnetic resonance imaging, *VIS*: macro-photography, *SEM*: scanning electron microscopy

– erosion boundary: the matrix completely disappears by dissolution or erosion.

An alternative explanation of the fronts is provided by Goa and Meury (7), who base their opinion on earlier work by Melia *et al.* (19). Melia *et al.* (19) studied partly hydrated HPMC tablets by cryo-SEM, and concluded that the gel layer is not homogeneous. This indicates that the water penetration is faster than the gel formation. Goa and Meury (7) adopt this result, and define the following boundaries, which they investigate by optical photography.

– The true penetration boundary: water has ingressed, but hardly any or no gel formation has taken place. Water thus ingresses through the glassy material, probably through pores in the (porous) carrier.
– The phase transition boundary: the glassy material is transformed to a gel matrix to such an extent that the matrix becomes transparent.
– The erosion boundary (dissolution front): the matrix completely disappears by dissolution or erosion.

The observed fronts are thus attributed to different physical processes. The inner front is seen by Goa and Meury (7) as the front where water has ingressed, but no gel has been formed yet. Colombo and colleagues (6) do not attribute a front to this process. On the other hand, Colombo attributes a front to the dissolution of the drug; a process that is, in the opinion of Goa and Meury (7), not visible as a front.

No convincing proof of either of these hypotheses has been found in literature. Nevertheless, it is clear that the boundaries observed in photography are sharp, unlike the fluent gradients obtained from mathematical simulation based on Fick's laws (21–23) and the results of FTIR spectroscopic imaging (12,13,15,17,24). This can be attributed to the fact that photography does not provide a quantitative value for the concentration of the different materials. Rather, it shows effects that occur at a specific concentration. For example, water imbibition into a tablet causes the pores of a tablet to be filled, leading to a reduction of the refractive index changes, reduction of scattering and thus a sharp front. Further imbibition gradually increases the water concentration, but it is assumed that this is not observed in photography, unless a further physical change occurs, such as the conversion from a glassy to a gel matrix, or the erosion of the tablet. Photography is thus well suited to localise the physical changes in the tablet. Unfortunately, the observation of a boundary does not make its interpretation obvious, which explains the above controversial explanation of the different fronts.

As explained, both MRI and macro-photography do not yield accurate quantifications in the described application. The main challenge is to quantify all different components of the system (matrix, drug, water) with a high spatial and temporal resolution. Such a complete dissolution set (c_i (x,y, z,t), i.e. the concentrations of all components as a function of space and time), would enable the evaluation of the different hypotheses put forward to describe the fronts observed in macro-photography.

Therefore, we aimed to devise a tablet dissolution cell that enables the simultaneous acquisition of photographic and FTIR spectroscopic imaging data. The ATR approach was selected rather than the transmission mode as it eliminates the need for very thin tablets, and makes the technical design of a set-up easier. Studies with such a cell would yield an accurate quantification of all relevant compounds in the surface layer adjacent to the ATR crystal, and a description of the various boundaries observed in photography during tablet dissolution.

The current paper describes the method to combine ATR-FTIR imaging and macro-photography. Tablets can be studied by these techniques simultaneously. Results of the hyphenated technique will be used to clarify the issue regarding the physical origin of the fronts.

On a longer time-scale, the developed technique may be an aid to validate and improve mathematical models and

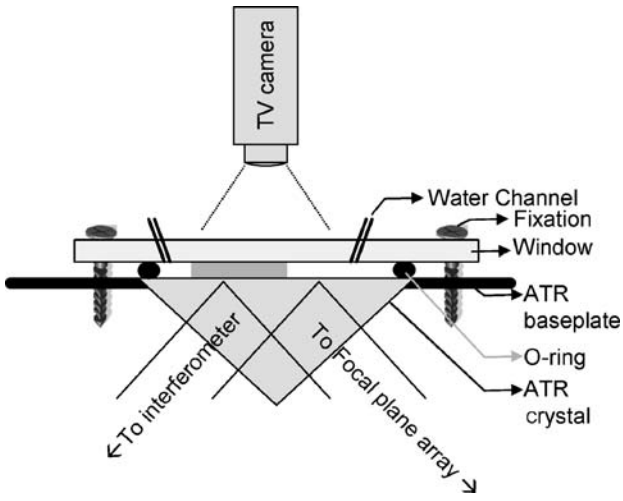

Fig. 1. Schematic presentation of the developed tablet cell.

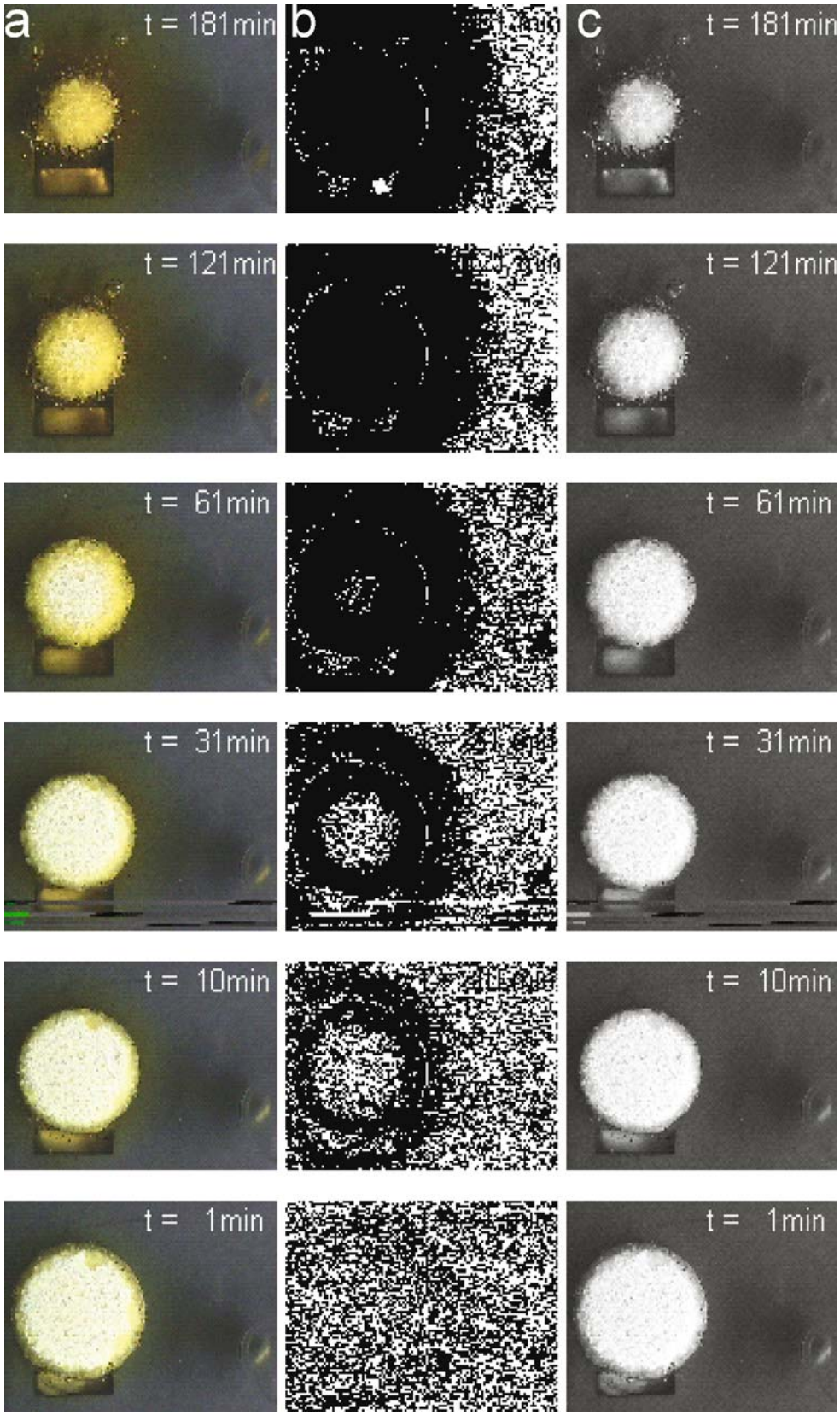

Fig. 2. Selection of visible light images acquired during tablet dissolution. *White numbers in the images* indicate the time since the exposure to water started. **a** Raw images. **b** Images optimised to highlight both the inner and outer fronts. See text for the used procedure. **c** Images optimised to highlight the middle front by summation of the three colour channels.

hence reduce the time and costs to develop a tablet with specific release characteristics.

CELL DESIGN CONSIDERATIONS

The construction of the proposed cell (Fig. 1) is based on a previous cell (14) made specifically for FTIR imaging studies. The prominent feature of that cell was the possibility to compact tablets *in situ*, i.e. inside the measurement cell. The rationale for this was to minimise surface effects due to possible water leakage into the interface between tablet and ATR crystal. However, later studies showed that leakage is not an issue for HPMC tablets (15), as a result of the swelling of HPMC matrix on water intake. Therefore, the current design does not have a facility to compact tablets *in situ*. Instead, tablets have to be compacted off-line.

The proposed tablet cell consists of an ATR accessory (Golden Gate) onto which a transparent polymer window is fixed. The tablet is clamped between the ATR crystal and the window. It is surrounded by an O-ring slightly thicker than the tablet, so that a sealed compartment is formed. A flow of water through this cell can be established via two channels in the window. These channels can be connected to ordinary tubing. ATR-FTIR spectra are acquired as described previously (17), while optical images can be acquired simultaneously through the window using a CCD camera (indicated as a TV camera in Fig. 1).

The set-up can be used as a flow-through dissolution test by determining the amount of drug in the solution after contact with the tablet (17). This is possible by any flow-through detector, such as the detectors used in high-pressure liquid chromatography.

MATERIALS AND METHODS

Materials. Drug: buflomedyl pyridoxal phosphate (BPP), a coloured drug, was kindly provided by Profs. Colombo and Bettini, HPMC (K4MRC) was kindly provided by Colorcon (Orpington Kent).

Instruments. FTIR imaging set-up used in these studies was described elsewhere (14). The used system has a time resolution of about 2 min, a FOV of about 820×1,140 μm^2, and a spatial resolution of about 20 μm (13). The imaging ATR spectrometer has been patented by Varian (25). A Colour Video Camera (Sony Exwave HAD), interfaced to a DT313 Frame Grabber (Data Translation) image acquisition board was used to acquire visible images. Images were analysed using Matlab (version 7, the Mathworks).

Analysis. A mixture containing 60% BPP in hydroxypropyl methylcellulose (HPMC) was ground for several minutes using mortar and pestle. Part of the mixture was placed in a home-made mould (∅ 3 mm) and compacted at 5 kN using a calibrated torque wrench. The tablet was removed from the mould manually and placed on the measuring surface of a diamond crystal in a Golden Gate (Specac, Orpington, Kent, UK) ATR accessory, so that the tablet covers half the field of view (FOV). The tablet is surrounded by an O-ring and covered by a transparent top-plate, to which two tubes are connected. Distilled water is pumped through the cell at 1 ml/min using a HPLC pump (Kontron 332). The data acquisition (VIS and IR) is started as soon as the tablet cell is filled with water. FTIR data are acquired automatically using a macro in the acquisition spectroscopic software. VIS images are acquired using the image acquisition toolbox in Matlab.

Data-processing. Optical images and FTIR datasets are processed using home written procedures in Matlab.

RESULTS

Macro-photography

A selection of the acquired optical images is presented in Fig. 2a (left column). At the start of the experiments (bottom image), the tablet appears white due to scattering of the white tablet matrix (HPMC). The square seen below the tablet is the surface of the prism-shape diamond ATR crystal used for the FTIR imaging experiments. In due time, the drug dissolves and the scattering decreases due to gel formation. In addition, the colour of the tablet turns yellow-orange due to dissolution of BPP.

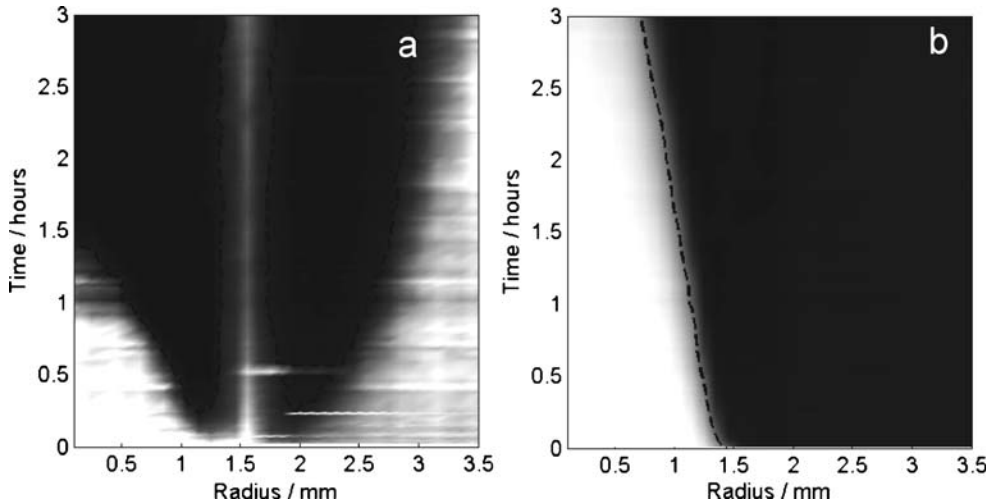

Fig. 3. Evolution of the three fronts observed in macro-photography. **a** Fronts derived from plots in Fig. 2b. **b** Front derived from plots in Fig. 2c. See text for calculations.

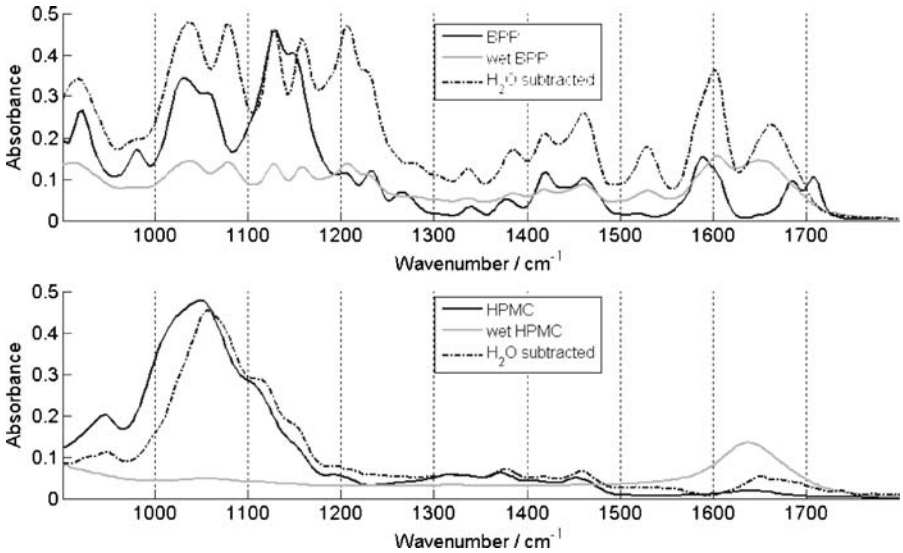

Fig. 4. FTIR spectra of HPMC and BPP, both wet and dry. The spectra of the wet material have been corrected for water absorptions, and formed the basis of the CLS set used to calculate concentrations from the infrared spectra in the FTIR-ATR imaging sets.

A number of boundaries can be seen in the images. The first front, between the white inner part and the yellow rim, is seen moving inward at a relatively high speed until it reaches the centre of the tablet at around 121 min. The apparent outer radius of the tablet is seen moving inward more slowly. At 181 min, the radius of the tablet is reduced to about half the original value. A third area can be recognised around the white/yellow core by a pale yellow colour. The outer boundary of this transparent gel-layer cannot readily be seen from the pictures in Fig. 2a. Closer inspection reveals the presence of a pale yellow boundary moving outward.

This series of images was used to derive the position of the fronts as a function of time. An algorithm capable of this task has been described before (16). It simplifies the data-set by summarising the two image dimension (X, Y) to a single dimension, (radius) and is based on the assumption of circular symmetry. In short, the algorithm finds all pixels at a certain radius, and averages the values in these pixels. In the current version, the algorithm only accepts a time series of univariate data, so colour images (containing 3 channels) need to be pre-processed. This pre-processing has to be carried out in such a way that the important fronts are highlighted. The core of the tablet (yellow/white parts) can easily be highlighted by summation of the three channels, as shown in Fig. 2c. Highlighting the other, more subtle fronts appeared possible by selecting the blue channel (orange drug, so a reduction of the blue light level may be expected). Furthermore, the starting image (t=0) was subtracted from this series. Samples of the resulting series of images are shown in Fig. 2b. These images are noisy because they show a difference rather than the total observed intensity. Nevertheless, they localise the two boundaries with a good accuracy and contrast.

The two series of pre-processed images (Fig. 2b and c) were processed using the algorithm described above. The results are shown in Fig. 3. In these plots, the x-axis describes the radius of the tablet, the y-axis describes the time evolution, and the intensity of the image elements represents

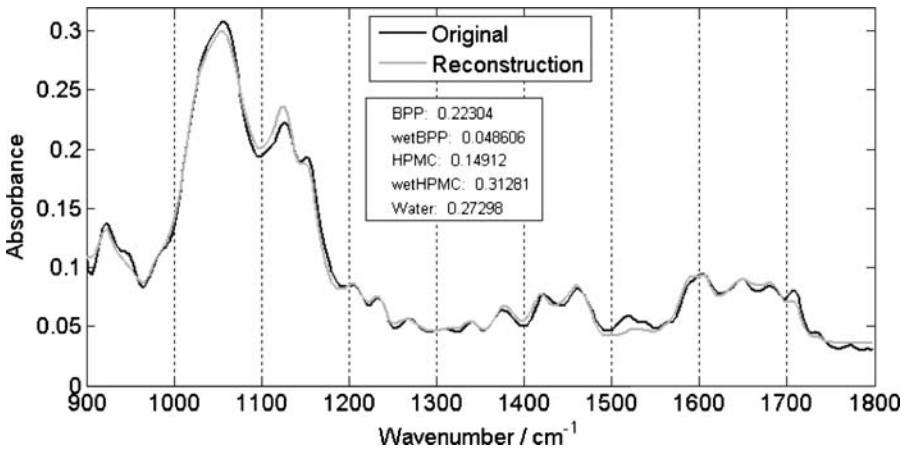

Fig. 5. Comparison of reconstructed and acquired reference spectra for validation of the CLS procedure.

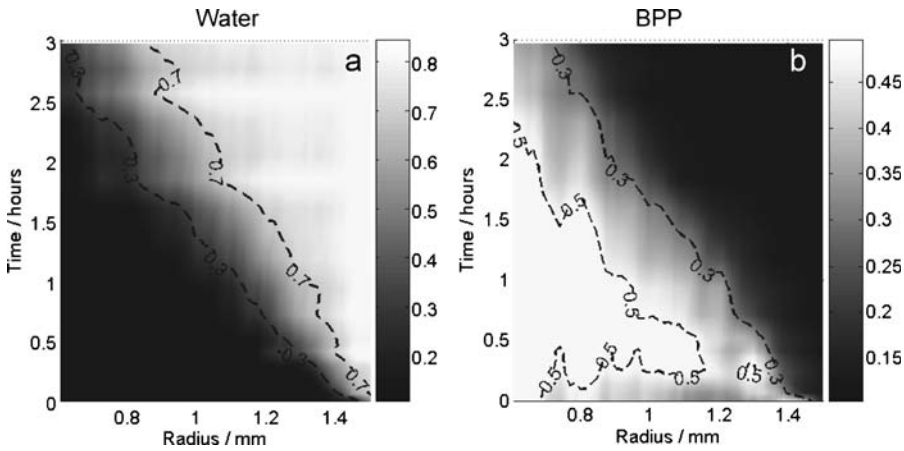

Fig. 6. Results of FTIR-ATR imaging. The obtained imaging data-sets have been processed using CLS. The concentration of different components as function of radius was than calculated as described in the texts. The dashed lines connect points of equal concentration in these profiles. **a** Concentration profiles for the amount of water. **b** Concentration profiles for BPP.

the average of all pixels at a specific radius and time, as seen in Fig. 2b and c. The dashed lines in this plot connect points of equal greyscale. This line indicates the movement of the fronts, and will be used below.

FTIR Imaging

In this section, the procedures described above will be applied to the FTIR imaging datasets obtained simultaneously with optical (VIS) datasets by photography. Obviously, the differences between the VIS and the FTIR imaging experiments require some adjustments, but the principles are essentially the same.

As described above, the datasets need to be reduced to a time series of 2D sets. The FTIR datasets contain a complete spectrum for every pixel, rather than three variables per pixels for VIS datasets. The highly specific and quantitative nature of IR spectroscopy allows summarising datasets to a few numbers, namely the concentrations of the present materials. In fact, this is rather straightforward, as all involved components are available as pure materials. Reference IR spectra of these materials were acquired and used as a calibration set for classical least squares (CLS) processing. The included spectra are shown in Fig. 4. It appeared necessary to include spectra of both wet and dry reference materials, as the spectra of BPP and HPMC were altered significantly due to the interaction with water. The spectra of the wet materials were corrected for the absorption of water. The quality of the CLS fitting can be evaluated by fitting errors or, more visually, by comparing original spectra to spectra reconstructed from the reference spectra and the calculated concentrations. Figure 5 shows such a comparison for one of the >90,000 acquired spectra. No systematic errors were found in many such comparisons, and the results were used in further processing.

CLS summarises every spectrum in a few numbers, namely the relative concentrations of the relevant materials. If a single material is selected, a time series of 2D images is obtained. These series (not shown) can be used to calculate the concentration as a function of time and radius using the algorithm described above. The resulting images are shown in Fig. 6. These images are directly comparable to the images in Fig. 3, be it that the field of view (FOV) is adjusted due to the altered acquisition method. The ingression of water is seen in Fig. 6a. It can be seen that a gradual transition from the dry core to the surrounding water fraction is established,

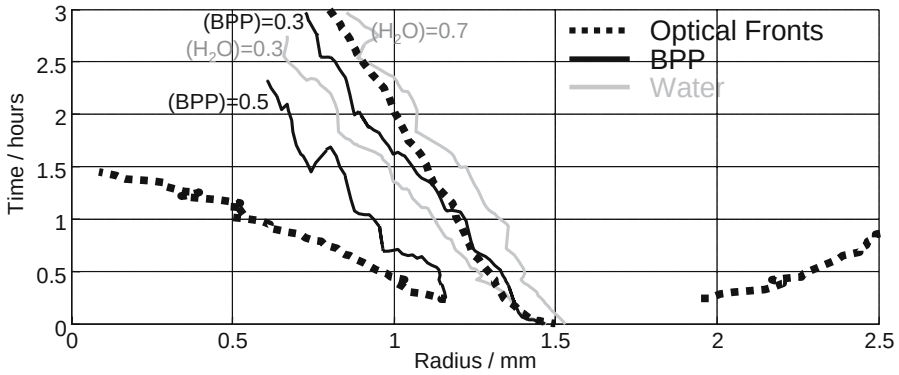

Fig. 7. Combined results of macro-photography and FTIR-ATR imaging. The *dashed lines* show the three fronts as presented in Fig. 3. The *solid lines* show the points of equal concentration shown in Fig. 6. The concentrations are provided as fractions.

which is indicative of a continuous swelling/dilution of the gel layer. Two dashed lines are shown in this figure, indicating at what time and radius the tablet contained about 30 % and 70 % water. These lines are surprisingly straight, but comparable to profiles reported before (15).

Figure 6b shows the concentration of BPP as a function of time and radius. Again, a gradual transition from the highly loaded tablet core to the empty surroundings is observed. Early in the experiment (t<20 min), deviations are seen in this image due to the imperfect contact between the dry tablet and the ATR crystal. At later times, swelling improves the contact. A number of dashed lines are drawn in Fig. 6b. These connect points of equal BPP content.

DISCUSSION

Figure 7 summarises the information shown in Figs. 3 and 6. Dashed lines in Fig. 7 are the fronts observed in VIS photography (Fig. 3), The rates of all three visible fronts are consistent with earlier studies, in which a similar tablet composition was used (6), which indicates that analyses of the newly developed tablet cell can well be compared to analyses focussing only on macro-photography.

The solid lines in Fig. 7 are the profiles derived from the FTIR spectroscopic analyses (Fig. 6). The innermost front observed in VIS photography is located at positions where the water concentration is still low ($\ll$0.3). Accordingly, attribution to the gel-formation seems unlikely. Rather, this front should be attributed to the 'true penetration front', i.e. water penetrating through the channels inside the porous tablet with no or partial gelling of HPMC. This phenomenon has been reported before (15). This process may well be accompanied by a fast dissolution of the (well soluble) BPP, and thereby leads the yellowing observed at this front (Fig. 3b). It seems reasonable to assume that BPP dissolves partly within seconds after exposure to water.

The second front observed in VIS photography occurs at a water content between 0.3 and 0.7(approximately 0.6). It seems the most likely to attribute this front to the transformation of glassy polymer to gel. The deviation from the theoretical value for gel formation (~20% water (26)) can be explained by the time needed for gelling. This attribution is confirmed by the large reduction in the visibility of the polymer (Fig. 3b). The outer front observed in VIS photography is outside the FOV in the FTIR imaging analyses. Nevertheless, it is clear that this front occurs at very high water content. It seems thus reasonable to attribute this front to erosion. This identification of the various fronts is consistent with the results by Gao and Meury (7) rather than with alternative hypotheses put forward (6).

CONCLUSION

We have developed a method to study dissolution of a tablet simultaneously by FTIR-ATR imaging and macro-photography. This method was demonstrated for particular example of HMPC/BPP tablet. From this combined approach, it was possible to attribute the fronts observed in photography of dissolution of this tablet to physical processes.

The three fronts observed (inside to outside) are concluded to be due to: (1) true water penetration, possibly combined with (partial) dissolution of BPP; (2) total gellification of HPMC; (3) erosion front. The correct assignment of these fronts is important for understanding of the mechanism of drug release from tablets based on HPMC.

This combined approach of "chemical" and visible photography promises to aid in understanding of tablet dissolution processes in similar systems for controlled drug delivery and may impact many areas of pharmaceutical research. Obviously, a correct understanding of the observations will not alter the release properties of a tablet. Rather, to take full advantage of this knowledge, it will have to be integrated with other experimental results into an accurate mathematical model and as such facilitate a better prediction of the properties of a specific tablet.

Direct observation of samples by both visible imaging and FTIR imaging will allow direct comparison of quantitative and chemically specific FTIR imaging data obtained from the bottom surface layer of the sample with the visible images obtained from the top surface of the sample.

ACKNOWLEDGEMENT

We thank EPSRC for support (Grant GR/503942). The Chemical Engineering workshop at Imperial College London is thanked for the help with the construction of the described cell.

REFERENCES

1. C. A. Fyfe and A. I. Blazek. Complications in investigations of the swelling of hydrogel matrices due to the presence of trapped gas. *J. Control. Release* **52**:221–225 (1998).
2. C. A. Fyfe and A. I. Blazek-Welsh. Quantitative NMR imaging study of the mechanism of drug release from swelling hydroxypropylmethylcellulose tablets. *J. Control. Release* **68**:313–333 (2000).
3. C. A. Fyfe, H. Grondey, A. I. Blazek-Welsh, S. K. Chopra, and B. J. Fahie. NMR imaging investigations of drug delivery devices using a flow-through USP dissolution apparatus. *J. Control. Release* **68**:73–83 (2000).
4. C. D. Melia, A. R. Rajabi-Siahboomi, and R. W. Bowtell. Magnetic resonance imaging of controlled release pharmaceutical dosage forms. *Pharm. Sci. Technol. Today* **1**:32–39 (2000).
5. P. Colombo, R. Bettini, P. Santi, A. De Ascentiis, and N. A. Peppas. Analysis of the swelling and release mechanisms from drug delivery systems with emphasis on drug solubility and water transport. *J. Control. Release* **39**:231–237 (1996).
6. R. Bettini, P. L. Catellani, P. Santi, G. Massimo, P. N. Peppas, and P. Colombo. Translocation of drug particles in HPMC matrix gel layer: effect of drug solubility and influence on release rate. *J. Control. Release* **70**:383–391 (2001).
7. P. Gao and R. H. Meury. Swelling of hydroxypropyl methylcellulose matrix tablets. 1. Characterization of swelling using a novel optical imaging method. *J. Pharm. Sci.* **85**:725–731 (1996).
8. P. Gao, J. W. Skoug, P. R. Nixon, T. R. Ju, N. L. Stemm, and K. C. Sung. Swelling of hydroxypropyl methylcellulose matrix tablets. 2. Mechanistic study of the influence of formulation variables on matrix performance and drug release. *J. Pharm. Sci.* **85**:732–740 (1996).
9. P. Colombo, R. Bettini, P. L. Catellani, P. Santi, and N. A. Peppas. Drug volume fraction profile in the gel phase and drug release kinetics in hydroxypropylmethyl cellulose matrices containing a soluble drug. *Eur. J. Pharm. Sci.* **9**:33–40 (1999).

10. J. Adler, A. Jayan, and C. D. Melia. A method for quantifying differential expansion within hydrating hydrophilic matrixes by tracking embedded fluorescent microspheres. *J. Pharm. Sci.* **88**:371–377 (1999).
11. G. S. Bajwa, K. Hoebler, C. Sammon, P. Timmins, and C. D. Melia. Microstructural imaging of early gel layer formation in HPMC matrices. *J. Pharm. Sci.* **95**:2145–2157 (2006).
12. S. G. Kazarian and K. L. A. Chan. "Chemical photography" of drug release. *Macromolecules* **36**:9866–9872 (2003).
13. K. L. A. Chan, S. V. Hammond, and S. G. Kazarian. Applications of attenuated total reflection infrared spectroscopic imaging to pharmaceutical formulations. *Anal. Chem.* **75**:2140–2146 (2003).
14. J. van der Weerd, K. L. A. Chan, and S. G. Kazarian. An innovative design of compaction cell for *in situ* FT-IR imaging of tablet dissolution. *Vib. Spectrosc.* **35**:9–13 (2004).
15. J. van der Weerd and S. G. Kazarian. Validation of macroscopic ATR-FTIR imaging to study dissolution of swelling pharmaceutical tablets. *Appl. Spectrosc.* **58**:1413–1419 (2004).
16. J. van der Weerd, and S. G. Kazarian. Release of poorly soluble drugs from HPMC tablets studied by FTIR imaging and flow-through dissolution tests. *J. Pharm. Sci.* **94**:2096–2109 (2005).
17. J. van der Weerd and S. G. Kazarian. Combined approach of FTIR imaging and conventional dissolution tests applied to drug release. *J. Control. Release* **98**:295–305 (2004).
18. C. A. Coutts-Lendon, N. A. Wright, E. V. Mieso, and J. L. Koenig. The use of FT-IR imaging as an analytical tool for the characterization of drug delivery systems. *J. Control. Release* **93**:223–248 (2003).
19. C. D. Melia, A. R. Rajabi-Siahboomi, and M. C. Davies. The development of structural features in the surface gel layer of hydrating HPMC hydrophilic matrices. *Proceed. Intern. Symp. Control. Rel. Bioact. Mater.* **19**:28–29 (1992).
20. C. D. Melia, A. R. Rajabi-Siahboomi, A. C. Hodsdon, J. Adler, and J. R. Mitchell. Structure and behaviour of hydrophilic matrix sustained release dosage forms: 1. The origin and mechanism of formation of gas bubbles in the hydrated surface layer. *Int. J. Pharm.* **100**:263–269 (1993).
21. J. Siepmann and N. A. Peppas. Modeling of drug release from delivery systems based on hydroxypropyl methylcellulose (HPMC). *Adv. Drug Deliv. Rev.* **48**:139–157 (2001).
22. B. Narasimhan. Mathematical models describing polymer dissolution: consequences for drug delivery. *Adv. Drug Deliv. Rev.* **48**:195–210 (2001).
23. F. A. Radu, M. Bause, P. Knabner, G. W. Lee, and W. C. Friess. Modeling of drug release from collagen matrices. *J. Pharm. Sci.* **91**:964–972 (2002).
24. D. W. Rafferty and J. L. Koenig. FTIR imaging for the characterization of controlled-release drug delivery applications. *J. Control. Release* **83**:29–39 (2002).
25. E. M. Burka, and R. Curbelo. Imaging ATR spectrometer. US Patent 6.141,100 (2000).
26. B. C. Hancock and G. Zografi. The relationship between the glass-transition temperature and the water-content of amorphous pharmaceutical solids. *Pharm. Res.* **11**:471–477 (1994).